

Spin-polarized pairing induced by the magnetic field in the Bernal bilayer graphene

Yan Huang(黄妍) and Tao Zhou(周涛)

Citation: Chin. Phys. B, 2024, 33 (**4**): 047403. DOI: 10.1088/1674-1056/ad102f
Journal homepage: http://cpb.iphy.ac.cn; http://iopscience.iop.org/cpb

What follows is a list of articles you may be interested in

Coexistence of antiferromagnetism and unconventional superconductivity in a quasi-one-dimensional flat-band system: Creutz lattice

Feng Xu(徐峰) and Lei Zhang(张磊)
Chin. Phys. B, 2024, 33 (**3**): 037402. DOI: 10.1088/1674-1056/acf5d2

Effects of carrier density and interactions on pairing symmetry in a t_{2g} model

Yun-Xiao Li(李云霄), Wen-Han Xi(西文翰), Zhao-Yang Dong(董召阳), Zi-Jian Yao(姚子健), Shun-Li Yu(于顺利), and Jian-Xin Li(李建新)
Chin. Phys. B, 2024, 33 (**1**): 017404. DOI: 10.1088/1674-1056/ad1094

Ultralow-temperature heat transport study of noncentrosymmetric superconductor CaPtAs

Yimin Wan(万一民), Erjian Cheng(程二建), Yuxin Chen(陈宇鑫), Chengcheng Zhao(赵成成), Chengpeng Tu(涂成鹏), Dongzhe Dai(戴东喆), Xiaofan Yang(杨小帆), Lu Xin(辛路), Wu Xie(谢武), Huiqiu Yuan(袁辉球), and Shiyan Li(李世燕)
Chin. Phys. B, 2023, 32 (**12**): 127403. DOI: 10.1088/1674-1056/ad02e9

Multi-band analysis on physical properties of superconducting FeSe films

Jian-Tao Che(车剑韬) and Chen-Xiao Ye(叶晨骁)
Chin. Phys. B, 2023, 32 (**9**): 097401. DOI: 10.1088/1674-1056/acd3e5

Flux pinning evolution in multilayer Pb/Ge/Pb/Ge/Pb superconducting systems

Li-Xin Gao(高礼鑫), Xiao-Ke Zhang(张晓珂), An-Lei Zhang(张安蕾), Qi-Ling Xiao(肖祁陵), Fei Chen(陈飞), and Jun-Yi Ge(葛军饴)
Chin. Phys. B, 2023, 32 (**3**): 037402. DOI: 10.1088/1674-1056/ac89e1

Spin-polarized pairing induced by the magnetic field in the Bernal bilayer graphene

Yan Huang(黄妍) and Tao Zhou(周涛)[†]

Guangdong Basic Research Center of Excellence for Structure and Fundamental Interactions of Matter, Guangdong Provincial Key Laboratory of Quantum Engineering and Quantum Materials, School of Physics, Guangdong–Hong Kong Joint Laboratory of Quantum Matter, and Frontier Research Institute for Physics, South China Normal University, Guangzhou 510006, *China*

(Received 13 September 2023; revised manuscript received 20 November 2023; accepted manuscript online 28 November 2023)

Recent experimental findings have demonstrated the occurrence of superconductivity in Bernal bilayer graphene when induced by a magnetic field. In this study, we conduct a theoretical investigation of the potential pairing symmetry within this superconducting system. By developing a theoretical model, we primarily calculate the free energy of the system with $\mathrm{p}+\mathrm{ip}$-wave parallel spin pairing, $\mathrm{p}+\mathrm{ip}$-wave anti-parallel spin pairing and $\mathrm{d}+\mathrm{id}$-wave pairing symmetry. Our results confirm that the magnetic field is indeed essential for generating the superconductivity. We discover that the $\mathrm{p}+\mathrm{ip}$-wave parallel spin pairing leads to a lower free energy for the system. The numerical calculations of the energy band structure, zero-energy spectral function and density of states for each of the three pairing symmetries under consideration show a strong consistency with the free energy results.

Keywords: superconductivity, magnetic field induction, pairing symmetry, Bernal bilayer graphene

PACS: 74.70.Wz, 71.70.Ej, 74.20.Rp **DOI:** 10.1088/1674-1056/ad102f

1. Introduction

Graphene is a single-layer carbon atom crystal composed of two types of closely arranged carbon atoms.[1] This structure endows it with many unique physical properties,[2,3] making it widely applicable in various fields. In addition to single-layer graphene, multi-layer graphene has also attracted extensive research interest.[4–21] Since the first production of graphene in 2004,[22] achieving superconductivity in graphene-based two-dimensional materials has garnered considerable attention.[21,23–32]

One pioneering discovery was the observation of unconventional superconductivity in magic-angle graphene superlattices in 2018. For twist angles of about 1.1°, the electronic band structure of this system exhibits flat bands near the Fermi energy, resulting in correlated insulating states at half-filling. Superconductivity emerges upon doping this correlated insulating state.[21] Moreover, numerous studies have shown that graphene's superconductivity can be controlled by adjusting external conditions, including using hydrostatic pressure to controllably tune the interlayer separation in van der Waals heterostructures, offering a dynamic way to modify electronic properties. In graphene encapsulated in boron nitride, researchers observe that increasing pressure produces a superlinear increase in the moiré-superlattice-induced bandgap.[30] In addition, electric field-tunable superconductivity has been discovered in alternating-twist magic-angle trilayer graphene.[31] Recently, experiments have also shown that placing monolayer tungsten diselenide on Bernal-stacked bilayer graphene could promote Cooper pairing, with superconductivity appearing at zero magnetic field.[8,9]

In recent years, two types of graphene trilayers have been proven to demonstrate unconventional superconductivity. One of them is rotationally faulted[32] and the other is in a metastable rhombohedral stacking order.[33] Both exhibit superconducting states above the paramagnetic limit, indicating the possible spin-triplet superconductor. However, these two materials are not the structural ground state and the many difficulties encountered in their manufacturing and operating processes impede further research. Recently, magnetic field-induced superconductivity in Bernal bilayer graphene (BBG) was reported. This superconducting state also exists above the paramagnetic limit and has been considered as spin-polarized superconductivity.[34] The crystal structure of BBG is similar to the graphene trilayer in a metastable rhombohedral stacking order, but it is more stable, providing greater operability in experiments.

Although superconductivity has been observed in BBG, the pairing mechanism remains unclear, sparking extensive theoretical research.[18,35–42] In fact, the superconducting pairing symmetry of this spin-triplet system has not been further confirmed. Therefore, revealing the physical characteristics of BBG under different superconducting pairing symmetries is of great significance for verifying and comparing them experimentally in the future.

In this paper, we theoretically study the physical characteristics of superconductivity in BBG with different pairing symmetries. We consider three different pairing symmetries,

[†]Corresponding author. E-mail: tzhou@scnu.edu.cn

© 2024 Chinese Physical Society and IOP Publishing Ltd

namely, the p+ip-wave with parallel spin pairing, p+ip-wave with anti-parallel spin pairing and the d+id-wave pairing. First, we compute and compare the free energy of the system with these three different pairing symmetries and then calculate the energy band structure, zero-energy spectral function and density of states (DOS), respectively, intending to provide a theoretical reference for future experiments.

The rest of the paper is organized as follows. In Section 2, we introduce the model and present the corresponding formalism. In Section 3, we report the numerical calculations and discuss the obtained results. Finally, we provide a brief summary in Section 4.

2. Model and formalism

The Hamiltonian H of the superconducting BBG system in the momentum space can be written as $H=\sum_{\boldsymbol{k}}\Psi_{\boldsymbol{k}}^{\dagger}H_{\boldsymbol{k}}\Psi_{\boldsymbol{k}}$. $\Psi_{\boldsymbol{k}}^{\dagger}$ is a 16th-order vector, expressed as

$$\Psi_{\boldsymbol{k}}^{\dagger}=\left(C_{l,\boldsymbol{k},\uparrow}^{\dagger}\ C_{l,\boldsymbol{k},\downarrow}^{\dagger}\ C_{l,-\boldsymbol{k},\uparrow}\ C_{l,-\boldsymbol{k},\downarrow}\right), \tag{1}$$

with $l=1,2,3,4$ corresponding to two graphene layers and two sublattices for each layer, and $\boldsymbol{k}$ is the wavevector.

The 16×16 matrix $H_{\boldsymbol{k}}$ is expressed as

$$H_{\boldsymbol{k}}=\begin{pmatrix}H_0(\boldsymbol{k}) & H_{\Delta}(\boldsymbol{k})\\ H_{\Delta}^{*}(\boldsymbol{k}) & -H_0(-\boldsymbol{k})\end{pmatrix}, \tag{2}$$

where $H_0(\boldsymbol{k})$ is the particle part of the Hamiltonian and the $H_{\Delta}(\boldsymbol{k})$ stands for the superconducting part. $H_0(\boldsymbol{k})$ can be written as

$$\begin{aligned}H_0(\boldsymbol{k}) \ =\ & \sigma_0\otimes\left(-m\sigma_z\otimes\sigma_0+H_{\mathrm{g}}(\boldsymbol{k})\right)\\ &+\sigma_z\otimes(s_z\sigma_0\otimes\sigma_0)+\sigma_x\otimes(s_x\sigma_0\otimes\sigma_0),\end{aligned} \tag{3}$$

where m is the interlayer potential.[34] Experimentally, superconductivity arises in bilayer graphene when an additional magnetic field is applied parallel to the graphene plane. The parallel magnetic field can lead to magnetic states with $\langle S_{\alpha}\rangle\neq0$, resulting from the Zeeman effect, where S_{α} represents the α-component of the spin operator $\boldsymbol{S}$, and $\boldsymbol{S}=(S_x,S_y,S_z)$. In this study, the Hamiltonian is expressed using the S_z representation. The Zeeman field in the z-direction is represented as a spin-polarized term [s_z term in Eq. (3)], while the Zeeman field in the x- or y-direction is represented as a spin-flip term [s_x term in Eq. (3)]. It is important to note that the z-direction Zeeman field should also exist even when the magnetic field is along the in-plane direction.[43] In this work, we have numerically verified that the z-component Zeeman field is crucial for inducing superconductivity in the bilayer graphene compound. Here, without loss of generality, the Zeeman field includes both the z-component and the x-component. The parameters are chosen as $s_z=s_x=0.03$, $m=0.025$. σ_0 is the identity matrix, σ_z and σ_x are Pauli matrices. $H_{\mathrm{g}}(\boldsymbol{k})$ is a 4×4 matrix, which describes an accurate tight-binding model for AB stacked bilayer graphene with the hopping parameters being taken from Ref. [44].

The $H_{\Delta}(\boldsymbol{k})$ is the superconducting term matrix. For the spin singlet pairing symmetry (d+id-pairing symmetry), the two pairing electrons have the opposite-spin-orientation along the z-direction with $S_z=0$. However, for the spin triplet pairing symmetry (p+ip pairing symmetry), there are two different pairing forms, namely, in the $S_z=0$ channel or the $S_z=\pm1$ channel. In the $S_z=0$ channel, the two pairing electrons have the opposite-spin-orientation along the z-direction. Then we have

$$H_{\Delta}(\boldsymbol{k})=\begin{pmatrix}0 & H_{\mathrm{t}}(\boldsymbol{k})\\ -H_{\mathrm{t}}(\boldsymbol{k}) & 0\end{pmatrix}. \tag{4}$$

In the $S_z=\pm1$ channel, the two pairing electrons have the same spin orientation along the z-direction. Thus we have

$$H_{\Delta}(\boldsymbol{k})=\begin{pmatrix}H_{\mathrm{t}}(\boldsymbol{k}) & 0\\ 0 & H_{\mathrm{t}}(\boldsymbol{k})\end{pmatrix}. \tag{5}$$

Here, $H_{\mathrm{t}}(\boldsymbol{k})$ is expressed as

$$H_{\mathrm{t}}(\boldsymbol{k})=\begin{pmatrix}0 & \Delta(\boldsymbol{k}) & 0 & 0\\ \xi\Delta(-\boldsymbol{k}) & 0 & 0 & 0\\ 0 & 0 & 0 & \Delta(\boldsymbol{k})\\ 0 & 0 & \xi\Delta(-\boldsymbol{k}) & 0\end{pmatrix}. \tag{6}$$

Here, $\xi=1$ and $\xi=-1$ are for the spin triplet pairing and the spin singlet pairing, respectively. $\Delta(\boldsymbol{k})$ is the momentum-dependent superconducting pairing, expressed as

$$\Delta(\boldsymbol{k})=\sum_{j=1}^{3}\Delta_j\mathrm{e}^{\mathrm{i}\boldsymbol{k}\cdot\boldsymbol{e}_j}, \tag{7}$$

where

$$\begin{aligned}&\boldsymbol{e}_1=\frac{1}{\sqrt{3}}(0,1),\quad \boldsymbol{e}_2=\frac{1}{2\sqrt{3}}(\sqrt{3},-1),\\ &\boldsymbol{e}_3=\frac{1}{2\sqrt{3}}(-\sqrt{3},-1),\end{aligned}$$

and $\Delta_{1,2,3}=\Delta_0(1,\mathrm{e}^{\mathrm{i}2\pi/3},\mathrm{e}^{\mathrm{i}4\pi/3})$.

Consider a nearest-neighbor attractive interaction V as the pairing strength. The free energy can be expressed as

$$F=k_{\mathrm{B}}T\sum_{\eta}\ln[1-f(E_n)]-\mu N+\frac{\sum_i\Delta_{ii}^2}{V}, \tag{8}$$

where μ is the chemical potential, N is the particle number and $f(E_n)$ is the Fermi distribution of the system. The order parameter Δ_0 can be obtained self-consistently by minimizing the free energy, with

$$\frac{\partial F}{\partial\Delta_0}=0. \tag{9}$$

The Green's function matrix can be obtained by diagonalizing the Hamiltonian, with the elements being expressed as

$$G_{ij}(\boldsymbol{k},\omega)=\sum_n\frac{u_{in}(\boldsymbol{k})u_{jn}(\boldsymbol{k})^*}{\omega-E_n+\mathrm{i}\Gamma}, \tag{10}$$

where E_n and $u_{in}(\boldsymbol{k})$ are the eigenvalues and eigenvectors of the Hamiltonian matrix. Γ is a small quantity with $\Gamma = 0.001$. Then we can obtain the spectral function as

$$A(\boldsymbol{k},\omega) = -\frac{1}{\pi}\sum_{i=1}^{8}\mathrm{Im}G_{ii}(\boldsymbol{k},\omega). \tag{11}$$

The DOS can be calculated through the spectral function, with

$$\rho(\omega) = \frac{1}{N}\sum_{\boldsymbol{k}}A(\boldsymbol{k},\omega). \tag{12}$$

3. Results and discussion

The electronic band structure of graphene exhibits unique properties because the parabolic band touching at the Dirac point is inherently unstable. Numerous investigations have shown that applying a perpendicular displacement field induces a band gap at the touching point,[7,34,45–48] with the gap's magnitude increasing concomitantly with the interlayer potential difference. Capitalizing on this characteristic behavior, the superconducting state of BBG was experimentally achieved by imposing a strong magnetic field at an interlayer potential difference of 50 meV.[34] Motivated by these experimental findings, we perform calculations on this material system using parameters consistent with the experimentally realized conditions.

The magnetic field-induced superconductivity in BBG is considered to possess a spin-polarized nature, as it can exhibit superconducting characteristics above the paramagnetic limit.[34] Consequently, constructing the superconducting order parameter incorporates p + ip-wave symmetry with spin-triplet pairing. As aforementioned, p + ip-wave symmetry has two different spin pairing methods, namely, parallel spin pairing and anti-parallel spin pairing. To investigate the pairing symmetry of this system, we calculated the relevant physical properties corresponding to the two spin-pairing methods and compared them with the d + id-wave case.

First, we calculate the free energy of the superconducting state with three different pairing symmetries in the absence of a magnetic field. The free energy F as a function of the order parameter Δ_0 was computed via Eq. (8) with $s_x = s_z = 0$, $V = 0.433$ and is displayed in Fig. 1(a). We observe that in the range of Δ_0 from 0 to 0.02, the three free energy curves exhibit an increasing trend and almost completely coincide. Moreover, the free energy reaches its minimum value at $\Delta_0 = 0$, indicating that superconductivity will not emerge. This finding is also consistent with previous research.[34] In cases where only the electric field is applied, the normal state energy bands of BBG become fully gapped, making it challenging for Cooper pairs to form and achieve superconductivity.

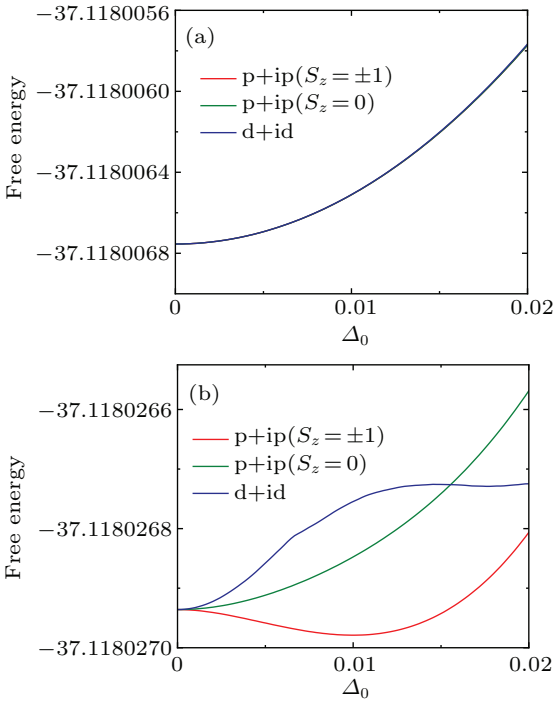


Fig. 1. (a) and (b) The free energy of superconducting states under three pairing symmetries before and after applying a magnetic field, respectively.

In the presence of a magnetic field, the numerical results of the free energy become significantly different, as seen in Fig. 1(b). Our results indicate that only the p + ip state in the $S_z = \pm 1$ channel can stabilize superconductivity. As shown, the free energy of the p + ip-wave with parallel-spin exhibits non-monotonic behavior, initially decreasing as Δ_0 grows from zero before passing through a minimum and increasing again at higher values of the order parameter. In contrast, the free energy of the p + ip-wave with anti-parallel spin pairing displays monotonic increasing behavior. Similarly, the d + id-wave pairing symmetry initially exhibits an increase, followed by a slight decrease before increasing again at higher Δ_0. The free energy of these two pairing states is higher than that of the normal state. Consequently, these two states will not be induced by the magnetic field. Upon examining the three pairings, the parallel-spin p + ip-wave pairing has the lowest overall free energy values. This comparison between pairing symmetries offers further evidence that the superconducting state in the BBG system likely exhibits p + ip-wave with parallel-spin pairing, as this configuration minimizes the free energy. Moreover, the magnetic field is necessary for generating superconductivity. Based on this conclusion, we aim to continue comparing the differences in other physical properties under the three pairing symmetries.

Using the effective magnetic field, we compute the normal state electronic band structure and Fermi surface topology via Eq. (3), which are displayed in Figs. 2(a) and 2(b), respectively. Figure 2(a) demonstrates that near the point K $[Q_K = (\frac{2\pi}{3a}, \frac{2\pi}{\sqrt{3}a})]$, the energy band crosses the Fermi energy, corresponding to the two nested Fermi pockets depicted in Fig. 2(b).

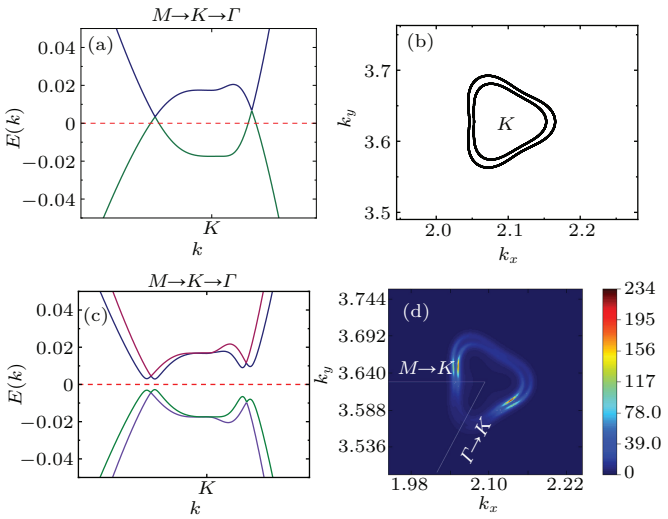


Fig. 2. (a) The normal state energy bands of BBG. (b) The Fermi surface topology of normal state around point-K in the Brillouin zone. (c) The energy bands of superconducting state with p + ip-wave with the parallel spin pairing channel, with $\Delta_0 = 0.01$. (d) The corresponding zero-energy spectral function in the superconducting state.

We now examine the physical properties in the superconducting state of the BBG system. The energy bands in the superconducting state for the p + ip-wave in the parallel spin pairing channel with $\Delta_0 = 0.01$ are illustrated in Fig. 2(c). A superconducting gap along the highly symmetric lines is revealed. Furthermore, the zero-energy spectral function $A(\boldsymbol{k}, 0)$ is computed using Eqs. (10) and (11). The intensity plot of the spectral function at zero energy $(A(\boldsymbol{k}, 0))$ near the K point of the Brillouin zone is displayed in Fig. 2(d). It is important to note that the entire normal state Fermi surface is not fully gapped, and energy nodes exist, resulting in a large zero-energy spectral function at the nodal region.

Subsequently, we calculate the superconducting state energy bands with the anti-parallel spin pairing channel and the corresponding zero-energy spectral functions; the results are presented in Fig. 3. For the p + ip-wave pairing symmetry, as seen in Figs. 3(a) and 3(b), an energy gap is opened along the highly symmetric lines, but the gap magnitude is significantly smaller than that in the parallel spin pairing channel. The normal state Fermi surface is also partially gapped, while the nodal region is larger. For the d + id-wave pairing symmetry, no energy gap is opened in the entire normal state Fermi surface. This result is in good agreement with the numerical result of the free energy shown in Fig. 1(b).

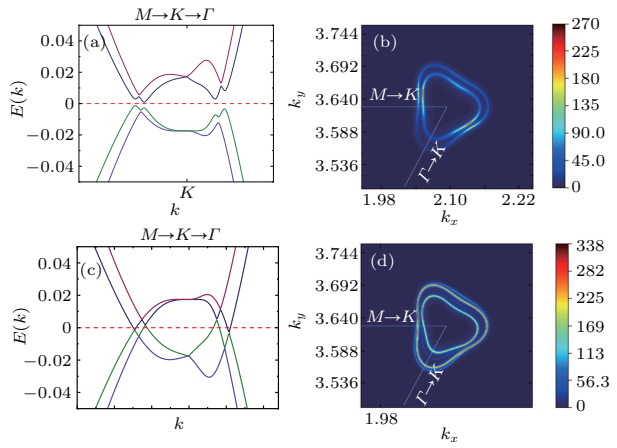


Fig. 3. (a) and (b) Energy bands and zero-energy spectral function of superconducting state with p-wave anti-parallel spin pairing symmetry ($\Delta_0 = 0.01$). (c) and (d) Energy bands and zero-energy spectral function of superconducting state with the d + id-wave pairing symmetry ($\Delta_0 = 0.01$).

The variations in physical properties exhibited by this material, due to different pairing symmetries, can be further investigated by calculating the DOS spectra [Eq. (12)]. These results are illustrated in Fig. 4. To compare the distinctions between the normal and superconducting states, we also display the numerical results of the normal state DOS with a dashed line. Figure 4(a) depicts the superconducting state DOS spectra for the two different p + ip-wave pairing symmetries. Owing to the opening of the energy gap and the presence of the nodal region, both low-energy DOS gap structures exhibit a "V"-shape. However, upon comparison, we observe that the DOS spectra corresponding to the p + ip-wave parallel spin pairing channel has a higher superconducting coherent peak and reduced energy distribution near zero energy.

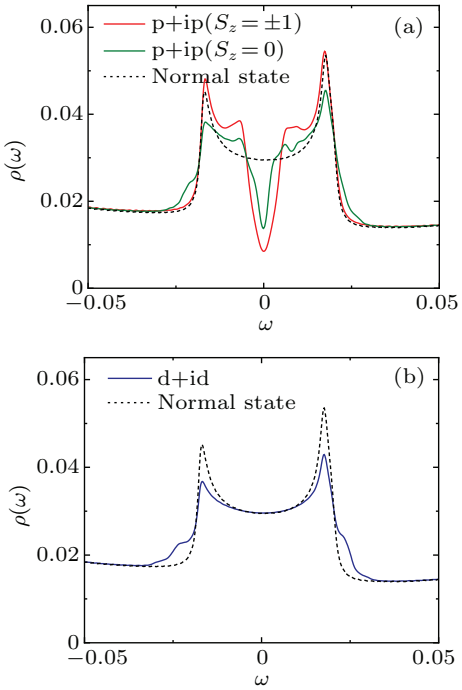


Fig. 4. The superconducting state DOS spectra for different pairing symmetry. The dashed lines are the DOS spectra in the normal state.

In Fig. 4(b), we plot the DOS spectra for the $d+id$-wave pairing symmetry. We note that for the $d+id$-wave pairing, there is no gap structure in the DOS spectrum, which aligns with the numerical results of the energy bands and zero-energy spectral function displayed in Fig. 3. The DOS near zero energy almost coincides with the spectra in the normal state. Our findings suggest that the differences between the $p+ip$-wave pairing and $d+id$-wave pairing can be readily distinguished experimentally through the DOS spectra.

4. Summary

In summary, we have conducted a theoretical study of the pairing symmetry of magnetic field-induced superconductivity in BBG. Considering the experimental conditions and the observed characteristics of the superconductor, we constructed and computed Hamiltonians based on three distinct pairing symmetries: $p+ip$-wave parallel spin pairing, $p+ip$-wave anti-parallel spin pairing, and $d+id$-wave pairing. Initially, we calculated the free energy of the superconducting state for these three pairing symmetries under both zero and finite magnetic field conditions. Our findings suggest that a magnetic field is essential for generating superconductivity, with the $p+ip$-wave parallel spin pairing exhibiting the lowest free energy. Subsequently, we utilized these results to compute the energy band structure, zero-energy spectral functions, and density of states spectra for the superconducting state associated with each of the three pairing symmetries. The ensuing calculations were in good agreement with our initial free energy conclusions. A comparative analysis of our results indicates that the spin-triplet superconducting state in BBG can be characterized by a $p+ip$-wave parallel spin pairing symmetry.

Acknowledgements

Project supported by the National Natural Science Foundation of China (Grant No. 12074130) and the Natural Science Foundation of Guangdong Province (Grant No. 2021A1515012340).

References

[1] Geim A K and Novoselov K S 2007 *Nat. Mater.* **6** 183
[2] Castro Neto A H, Guinea F, Peres N M R, Novoselov K S and Geim A K 2009 *Rev. Mod. Phys.* **81** 109
[3] Apell S P, Hanson G and Hägglund C 2012 arXiv:1201.3071
[4] Ghazaryan A, Holder T, Berg E and Serbyn M 2023 *Phys. Rev. B* **107** 104502
[5] Awoga O A, Löthman T and Black-Schaffer A M 2023 *Phys. Rev. B* **108** 144504
[6] Lu D C, Wang T, Chatterjee S and You Y 2022 *Phys. Rev. B* **106** 155115
[7] Shin J, Chittari B L, Jang Y, Min H and Jung J 2022 *Phys. Rev. B* **105** 245124
[8] Zhang Y, Polski R, Thomson A, Lantagne-Hurtubise É, Lewandowski C, Zhou H, Watanabe K, Taniguchi T, Alicea J and Nadj-Perge S 2023 *Nature* **613** 268
[9] Holleis L, Patterson C L, Zhang Y, Yoo H M, Zhou H, Taniguchi T, Watanabe K, Nadj-Perge S and Young A F 2023 arXiv.2303.00742
[10] Assouline A, Wang T, Zhou H, Cohen L A, Yang F, Zhang R, Taniguchi T, Watanabe K, Mong R S K, Zaletel M P and Young A F 2024 *Phys. Rev. Lett.* **132** 046603
[11] Lin J X, Wang Y, Zhang N J, Watanabe K, Taniguchi T, Fu L and Li J I A 2023 arXiv.2302.04261
[12] Niu R, Li Z, Han X, Qu Z, Ding D, Wang Z, Liu Q, Liu T, Han C, Watanabe K, Taniguchi T, Wu M, Ren Q, Wang X, Hong J, Mao J, Han Z, Liu K, Gan Z and Lu J 2022 *Nat. Commun.* **613** 6241
[13] Chou Y Z and Wu F and Das Sarma S 2022 *Phys. Rev. B* **106** L180502
[14] Xie M and Das Sarma S 2023 *Phys. Rev. B* **107** L201119
[15] Curtis J B, Poniatowski N R, Xie Y, Yacoby A, Demler E and Narang P 2023 *Phys. Rev. Lett.* **130** 196001
[16] Xie Y M, Lantagne-Hurtubise É, Young A F, Nadj-Perge S and Alicea J 2023 *Phys. Rev. Lett.* **131** 146601
[17] Dong Z, Davydova M, Ogunnaike O and Levitov L 2023 *Phys. Rev. B* **107** 075108
[18] Wagner G, Kwan Y H, Bultinck N, Simon S H and Parameswaran S A 2023 arXiv.2302.00682
[19] Ren Y N, Cheng Q, Sun Q F and He L 2022 *Phys. Rev. Lett.* **128** 206805
[20] Le N D and Jolicoeur T 2023 *Phys. Rev. B* **107** 125129
[21] Cao Y, Fatemi V, Fang S, Watanabe K, Taniguchi T, Kaxiras E and Jarillo-Herrero P 2018 *Nature* **556** 43
[22] Novoselov K S, Geim A K, Morozov S V, Jiang D E, Zhang Y, Dubono, S V, Grigorieva I V and Firsov A A 2004 *Science* **306** 666
[23] Tonnoir C, Kimouche A, Coraux J, Magaud L, Delsol B, Gilles B and Chapelier C 2013 *Phys. Rev. Lett.* **111** 246805
[24] Chichinadze D V, Classen L and Chubukov A V 2020 *Phys. Rev. B* **101** 224513
[25] Linder J, Black-Schaffer A M, Yokoyama T, Doniach S and Sudbø A 2009 *Phys. Rev. B* **80** 094522
[26] Ichinokura S, Sugawara K, Takayama A, Takahashi T and Hasegawa S 2016 *ACS Nano* **10** 2761
[27] Chapman J, Su Y, Howard C, Kundys D, Grigorenko A, Guinea F, Geim A, Grigorieva I and Nair R 2016 *Sci. Rep.* **6** 1
[28] Di Bernardo A, Millo O, Barbone M, Alpern H, Kalcheim Y, Sassi U, Ott A, De Fazio D, Yoon D, Amado M, Ferrari A C, Linder J and Robinson J W A 2017 *Nat. Commun.* **8** 14024
[29] Ludbrook B, Levy G, Nigge P, Zonno M, Schneider M, Dvorak D, Veenstra C, Zhdanovich S, Wong D, Dosanjh P, Straßer C, Stöhr A, Forti S, Ast C R, Starke U and Damascelli A 2015 *Proc. Natl. Acad. Sci. USA* **112** 11795
[30] Yankowitz M, Jung J, Laksono E, Leconte N, Chittari B L, Watanabe K, Taniguchi T, Adam S, Graf D and Dean C R 2018 *Nature* **557** 404
[31] Hao Z, Zimmerman A, Ledwith P, Khalaf E, Najafabadi D H, Watanabe K, Taniguchi T, Vishwanath A and Kim P 2021 *Science* **371** 1133
[32] Cao Y, Park J M, Watanabe K, Taniguchi T and Jarillo-Herrero P 2021 *Nature* **595** 526
[33] Zhou H, Xie T, Taniguchi T, Watanabe K and Young A F 2021 *Nature* **598** 434
[34] Zhou H, Holleis L, Saito Y, Cohen L, Huynh W, Patterson C L, Yang F, Taniguchi T, Watanabe K and Young A F 2022 *Science* **375** 774
[35] Li Z, Kuang X, Jimeno-Pozo A, Sainz-Cruz H, Zhan Z, Yuan S and Guinea F 2023 *Phys. Rev. B* **108** 045404
[36] Shavit G and Oreg Y 2023 *Phys. Rev. B* **108** 024510
[37] Szabó A L and Roy B 2022 *Phys. Rev. B* **105** L201107
[38] Cea T 2023 *Phys. Rev. B* **107** L041111
[39] Davis S M, Chou Y Z, Wu F and Das Sarma S 2023 *Phys. Rev. B* **107** 045426
[40] Chou Y Z, Wu F, Sau J D and Das Sarma S 2022 *Phys. Rev. B* **105** L100503
[41] Jimeno-Pozo A, Sainz-Cruz H, Cea T, Pantaleón P A and Guinea F 2023 *Phys. Rev. B* **107** L161106
[42] Dong Z, Chubukov A V and Levitov L 2023 *Phys. Rev. B* **107** 174512
[43] Wang Qian, Chen H Y, Hu C R and Ting C S 2006 *Phys. Rev. Lett.* **96** 117006
[44] Jung J and MacDonald A H 2014 *Phys. Rev. B* **89** 035405
[45] Weitz R T, Allen M T, Feldman B E, Martin J and Yacoby A 2010 *Science* **330** 812
[46] Mayorov A S, Elias D C, Mucha-Kruczynski M, Gorbachev R V, Tudorovskiy T, Zhukov A, Morozov S V, Katsnelson M I, Fal'ko V I, Geim A K and Novoselov K S 2011 *Science* **333** 860
[47] Bao W, Velasco J, Zhang F, Jing L, Standley B, Smirnov D, Bockrath M, MacDonald A H and Lau C N 2012 *Proc. Natl. Acad. Sci. USA* **109** 10802
[48] Freitag F, Trbovic J, Weiss M and Schönenberger C 2012 *Phys. Rev. Lett.* **108** 076602